Low, C. M. L., Drew, H. R., & Waring, M. J. (1984) *Nucleic Acids Res. 12*, 4865–4879.
Maki, A. H., & Co, T. (1976) *Biochemistry 15*, 1229–1235.
Maki, A. H., & Cha, T.-A. (1983) *Photochem. Photobiol. 2*, 1035–1055.
McGlynn, S. P., Azumi, T., & Kinoshita, M. (1969) *Molecular Spectroscopy of the Triplet State*, p 99, Prentice-Hall, Englewood Cliffs, NJ.
Quigley, G. J., Ughetto, G., van der Marel, G. A., van Boom, J. H., Wang, A. H.-J., & Rich, A. (1986) *Science 232*, 1255–1261.
Schmidt, J., Antheunis, D. A., & van der Waals, J. H. (1971) *Mol. Phys. 22*, 1–17.
Tsao, D. H. H., Casas-Finet, J. R., Maki, A. H., & Chase, J. W. (1989) *Biophys. J. 55*, 927–936.
Ughetto, G., Wang, A. H.-J., Quigley, G. J., van der Marel, G. A., van Boom, J. H., & Rich, A. (1985) *Nucleic Acids Res. 13*, 2305–2323.
van der Waals, J. H., & de Groot, M. S. (1967) *Magnetic Interactions Related to Phosphorescence*, in *The Triplet State* (Zahlan, A. B., Ed.) pp 101–132, Cambridge University Press, Cambridge.
Van Dyke, M. M., & Dervan, P. B. (1984) *Science 225*, 1122–1127.
van Egmond, J., Kohler, B. E., & Chan, I. Y. (1975) *Chem. Phys. Lett. 34*, 423–426.
Vincent, J. S., & Maki, A. H. (1965) *J. Chem. Phys. 42*, 865–868.
von Schütz, J. U., Zuclich, J., & Maki, A. H. (1974) *J. Am. Chem. Soc. 96*, 714–718.
Wakelin, L. P. G. (1986) *Med. Res. Rev. 6*, 275–340.
Wakelin, L. P. G., & Waring, M. J. (1976) *Biochem. J. 157*, 721–740.
Wang, A. H.-J., Ughetto, G., Quigley, G. J., Hakoshima, T., van der Marel, G. A., van Boom, J. H., & Rich, A. (1984) *Science 225*, 1115–1121.
Waring, M. J., & Wakelin, L. P. G. (1974) *Nature 252*, 653–659.
Williamson, M. P., Gauvreau, D., Williams, D. H., & Waring, M. J. (1982) *J. Antibiot. 35*, 62–66.
Yoshida, T., Kimura, Y., & Katagiri, K. (1968) *J. Antibiot. 7*, 465–467.

Structure of Colorado Potato Beetle Lipophorin: Differential Scanning Calorimetric and Small-Angle X-ray Scattering Studies†

Chihiro Katagiri,*,‡ Mamoru Sato,§ Stan de Kort,‖ and Yukiteru Katsube§

Biochemistry Laboratory, Institute of Low Temperature Science, Hokkaido University, Sapporo, Japan, Institute for Protein Research, Osaka University, Suita, Japan, and Department of Entomology, Agricultural University, Wageningen, The Netherlands

Received February 28, 1991; Revised Manuscript Received June 26, 1991

ABSTRACT: The structure of lipophorin, isolated from hemolymph of the Colorado potato beetle, was investigated by differential scanning calorimetry (DSC) and small-angle X-ray scattering. The DSC heating curves of intact lipophorin showed endothermic peaks that were similar to peaks obtained with the hydrocarbon fraction isolated from this lipophorin. The observed peaks correlated with the transition of the hydrocarbons from an ordered into a more disordered state. Changes in structure of the lipophorin particles with increasing temperature were also observed by small-angle X-ray scattering studies. The structural organization of lipophorin was further elucidated by simulation analysis, using a three-layered symmetrical sphere as a model. These studies revealed that lipophorin from the Colorado potato beetle is a sphere with a maximum diameter of 175 Å. The sphere is composed of three radially symmetrical layers of different electron densities. The outer layer (37.5–39.5 Å in thickness) is composed of phospholipid, apolipophorin I, and part of apolipophorin II. The middle layer (5–10 Å) contains diacylglycerol, the rest of apolipophorin II, and probably β-carotene. The core of the particle (40–45 Å) only contains hydrocarbons. This structure differs from another model, previously proposed for cockroach and locust lipophorins [Katagiri, C., Sato, M., & Tanaka N. (1987) *J. Biol. Chem. 262*, 15857–15861], in the small size of the middle layer. The volume of the middle layer correlated well with the low diacylglycerol content of this lipophorin.

Since lipids are not water soluble, lipoproteins are essential for transport within animals from the sites of synthesis, absorption, and storage to sites of utilization (Chino, 1985; Goldstein et al., 1985; Shapiro et al., 1988). Lipoproteins from different animals have basically a common molecular architecture. The surface is covered with hydrophilic groups of phospholipids and apoproteins, whereas the core contains apolar lipids (Edelstein et al., 1979; Katagiri et al., 1987). Despite the common structural organization, lipoproteins may vary in physiological function, chemical composition, and metabolism. Mammalian lipoproteins, classified by their buoyant density, transport mainly triacylglycerol and cholesterol esters and are metabolized in peripheral cells and liver (Goldstein et al., 1985). In insects, a circulating lipoprotein, named lipophorin, transports diacylglycerol, free cholesterol, and hydrocarbons. Phospholipids, a major lipid class in insect

† This work was supported in part by a research grant (01540586) from the Ministry of Education, Science and Culture of Japan.
* To whom correspondence should be addressed.
‡ Hokkaido University.
§ Osaka University.
‖ Agricultural University.

0006-2960/91/0430-9675$02.50/0

lipophorin, do not rapidly exchange between particle and tissues. They seemed to be a structural constituent of the "vehicle" itself, together with two apoproteins (apolipophorins I and II) (Katagiri & Chino, 1973; Downer & Chino, 1985).

Many studies have been carried out to determine the structural organization of lipophorins. The location of the apoproteins has been deduced from studies using proteases (Kashiwazaki & Ikai, 1985; Robbs et al., 1985) or antisera (Shapiro et al., 1984). The position of the phospholipid has been inferred from nuclear magnetic resonance studies (Katagiri, 1985) in combination with phospholipase A_2 treatment, whereas the hydrocarbons have been located by differential scanning calorimetry and nuclear magnetic resonance studies (Katagiri et al., 1985). In addition, lipophorins have been analyzed by small-angle X-ray scattering. These studies have resulted in the construction of a spherical model for cockroach and locust lipophorins (Katagiri et al., 1987). The sphere of 168 Å in diameter is composed of three radially symmetrical layers: an outer layer with apolipophorin I and phospholipid, a middle layer with diacylglycerol and apolipophorin II, and a core of hydrocarbons. However, silkworm lipophorin, which hardly contains hydrocarbons but only diacylglycerol (Chino et al., 1969), does not exhibit a three-layered structure, because the electron density of the particle center was found to be homogeneous.

Recently, we purified and characterized lipophorin from hemolymph of adult Colorado potato beetle (de Kort & Koopmanschap, 1987; Katagiri & de Kort, 1991). The particle weight of this lipophorin is about 5.74×10^5, and it is composed of two apoproteins, apolipophorin I (apoLp-I,[1] $M_r = 2.51 \times 10^5$) and apolipophorin II (apoLp-II, $M_r = 0.78 \times 10^5$), similar to the situation of other insect lipophorins (Chino, 1985; Shapiro et al., 1988). However, the lipid composition appeared to be unusual. Colorado potato beetle lipophorin had a high content of hydrocarbons and phospholipids but was poor in diacylglycerol. Such a diacylglycerol-poor hydrocarbon-rich lipophorin has never been reported before.

An unusual lipid composition is interesting from both the physiological and structural point of view, because diacylglycerol comprises the middle layer of insect lipophorins together with apoLp-II (Chino, 1985, Katagiri et al., 1987). In this paper, we investigate the structure of the Colorado potato beetle lipophorin by differential scanning calorimetry and small-angle X-ray scattering, and the results are compared with similar data obtained from cockroach and locust lipophorins.

Materials and Methods

Purification of Lipophorin. Lipophorin from the Colorado potato beetle, *Leptinotarsa decemlineata* Say, was purified by KBr density gradient centrifugation according to de Kort and Koopmanschap (1987).

Lipid Extraction and Analysis. Lipids were extracted from lipophorin and subjected to silicic acid column chromatography according to Katagiri et al. (1985). The purity of each fraction was examined by thin-layer chromatography.

Differential Scanning Calorimetry (DSC). All calorimetric measurements were performed with a high-sensitivity SSC/580 differential scanning calorimeter (Daini Seikosha Co., Tokyo) according to Katagiri et al. (1985).

For measurements on intact protein, lipophorin was suspended in 50 mM phosphate buffer (pH 6.0) containing 150 mM NaCl and 40% glycerol. Glycerol was added to prevent ice formation, and, compared with glycerol-free samples, this concentration of glycerol did not disturb phase behavior over the temperature range discussed in the present study. A 60-μL aliquot containing 5.2 mg of lipophorin was sealed hermetically in a silver pan. A 60-μL aliquot of buffer solution was also sealed and used as a reference. About 1 mg of each lipid class, separated by silicic acid column chromatography, was also subjected to this method.

Scanning was performed at a rate of 1 °C/min during heating and at 5 °C/min during cooling. Lipophorin samples were first cooled to −20 °C in DSC pans and kept for about 10 min before a heating scan was initiated. Three-cycle measurements were performed on lipophorin samples; at first, samples were heated from −20 to 55 °C and cooled to −20 °C, then they were heated to 100 °C and cooled to −20 °C, and finally they were heated to 100 °C. The lipid samples were cooled in the same way and heated to 60 °C.

Small-Angle X-ray Scattering Experiments. The X-ray scattering experiments were performed according to Katagiri et al. (1987). The X-ray source was a 0.4 × 8 mm spot on the copper anode of Philips fine-focus X-ray tube, which was operated with a Rigaku Denki D9C X-ray generator run at 40 kV (30 mA). The scattered X-rays were detected on a one-dimensional position-sensitive proportional counter (delay-line type). The width of each detector channel was 0.1265 mm on a multichannel analyzer. The sample-to-detector distance was 297.5 mm. The scattered X-rays were accumulated for 4000 s in the range of the scattering angles from 3.0×10^{-3} to 7.7×10^{-2} rad. The X-ray experiments were performed over a temperature range increasing from 0 to 50 °C. Before each measurement, samples were equilibrated for 10 min at the new adjusted temperature. The scattering intensities were measured with 10.0 mg of protein/mL of lipophorin throughout the present study, because no interparticle interference was observed at this concentration.

Data Reduction and Analysis. The collected data were subjected to data reduction and analysis to give independent scattering intensities, $I(s)$ as described in a previous paper (Katagiri et al., 1987). The scattering parameter s is defined by $s = 4\pi \sin \theta/\lambda$, where 2θ is the scattering angle and λ the wavelength of X-ray ($\lambda = 1.5418$ Å). The radius of gyration, R_g, and the zero-angle scattering profile, $I(0)$, were derived from the Guinier plot (Guinier & Fournet, 1955) of the scattering intensity data in a smaller angle region (Guinier region). Since the Guinier region was not clearly observed at 50 °C, the data at this temperature were removed for further data analysis. In the course of data analysis, the intraparticle pair-distance distribution function, $P(r)$, was calculated by a Fourier transform of the scattering intensity data (Pilz et al., 1979)

$$P(r) = \frac{1}{2\pi^2}\int_0^\infty I(s)\, sr \sin sr\, ds$$

Due to the finite resolution of the scattering parameter s, the $P(r)$ function was numerically integrated from $s = 0$ to $s = s_{max}$, where s_{max} is the largest measurable s value. To avoid the resultant artificial fluctuation of the function by the termination effect and also by the counting errors in $I(s)$, accurate intensity measurement was performed until the s_{max}, at which point the scattering from protein solution is almost the same as that from its buffer solution and thus comes to the background level completely. The maximum particle dimension D_{max} was calculated from the distance r, beyond which the $P(r)$ function has no significant values and eventually approaches zero.

[1] Abbreviations: apoLp, apolipophorin; D_{max}, maximum particle dimension; DSC, differential scanning calorimetry; ΔH, enthalpy change; R_g, radius of gyration; ρ, electron density.

Table I: Chemical Data of Colorado Potato Beetle Lipophorin[a]

	M_r	n (electrons)	v (Å^3)	ρ (e/Å^3)	weight (%)	N
apolipophorin I	2.51×10^5	1.35×10^5	2.99×10^5	0.450	42.6	1
apolipophorin II	0.78×10^5	0.42×10^5	0.93×10^5	0.450	13.3	1
phospholipid	757	419	1237	0.339	18.8	143
free cholesterol	386	216	602	0.359	1.2	18
diacylglycerol	601	334	1097	0.305	2.2	21
carotenoids	537	296	892	0.332	1.4	15
hydrocarbons	500	286	1027	0.279	20.5	235

[a] M_r, n, and v are the average weight, number of electrons and volume of each molecular species; $\rho = n/v$ is the electron density. The particle weight of Colorado potato beetle lipophorin is 5.74×10^5. Since two-thirds of carotenoids are not identified, the data of β-carotene, one-third of carotenoids, is used for those of carotenoids in this table.

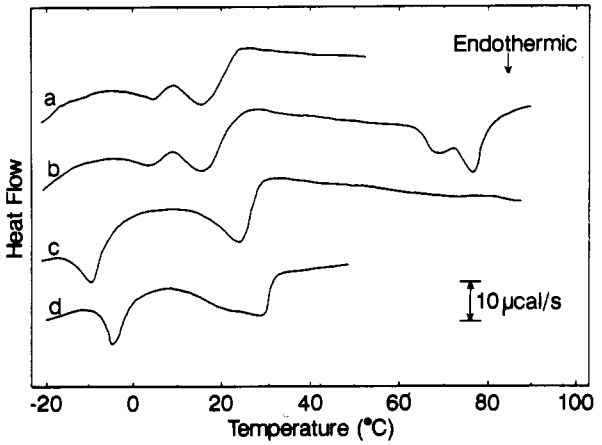

FIGURE 1: DSC heating curves of intact Colorado potato beetle lipophorin and of hydrocarbons isolated from Colorado potato beetle lipophorin. (a) Initial heating curve of intact lipophorin (5.2 mg of lipophorin in 60 μL of 50 mM phosphate buffer, pH 6.0, containing 40% glycerol) from −20 to 50 °C; (b) heating curve from −20 to 100 °C after cooling from 50 °C; (c) heating curve from −20 to 100 °C after cooling from 100 °C; (d) heating curve of hydrocarbons (1.1 mg) extracted from Colorado potato beetle lipophorin from −20 to 50 °C.

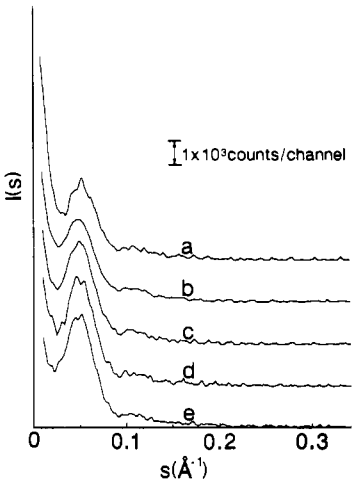

FIGURE 2: Small-angle X-ray scattering profiles of Colorado potato beetle lipophorin (10 mg of protein/mL) before the correction for slit smearing effect at the temperatures from 0 to 40 °C. (a) 0 °C; (b) 10 °C; (c) 20 °C; (d) 30 °C; (e) 40 °C.

Electron Microscopy. Lipophorin in 150 mM KCl was negatively stained with 1% uranyl acetate on collodion-coated grid supported by carbon and observed in a JEOL 1200EX electron microscope.

Results and Discussion

Differential Scanning Calorimetry. Typical DSC heating curves of intact lipophorin from Colorado potato beetle are illustrated in Figure 1 and demonstrate two groups of endothermic peaks, one between −5 and 9 °C and the other between 9 and 25 °C (Figure 1a), which are reversible on cooling (cooling curve not shown). The two groups of peaks are reproducible after reheating from −20 to 50 °C (Figure 1b). If the sample continues to be heated to 100 °C, other endothermic peaks appear between 60 and 80 °C (Figure 1b). The latter peaks were also observed with other insect lipophorins and proved to be due to denaturation of the apoproteins (Katagiri et al., 1985). When the samples are reheated to 100 °C after being cooled from 100 to −20 °C, the peaks between −5 and 25 °C are clearly separated: one between −18 and −5 °C and the other between 10 and 31 °C (Figure 1c). To determine which components of lipophorin contribute to these peaks, each lipid class was isolated from Colorado potato beetle lipophorin by silicic acid column chromatography and applied to DSC. Transitions between −20 and 50 °C were only observed with the hydrocarbon fraction (Figure 1d). The hydrocarbons extracted from lipophorin display two major peaks centered at −15 and 29 °C, respectively (Figure 1d), that resemble heat-denatured lipophorin (Figure 1c). If the peaks observed between −5 and 25 °C (Figure 1a,b) are due to the phase transition of the hydrocarbons, the ΔH of these peaks may give a similar value to that obtained from the solid–liquid transition of extracted hydrocarbons. The calculated ΔH of the peaks observed in Figure 1a is 4.4 cal/g of hydrocarbons, which is close to the value obtained with extracted hydrocarbons (5.0 cal/g of hydrocarbons). Therefore, similar to cockroach and locust lipophorins, the endothermic peaks observed between −5 and 25 °C represent the phase transition of hydrocarbons in Colorado potato beetle lipophorin, which suggests that Colorado potato beetle lipophorin also has a hydrocarbon-rich core. However, the question arises whether this lipophorin is composed of three layers similar to cockroach or locust lipophorin. The diacylglycerol content of Colorado potato beetle lipophorin (2% of total weight, Table I) is too low compared with cockroach and locust lipophorins (8 and 13% of total weight, respectively) to occupy the middle layer together with apoLp-II. Since DSC studies do not answer this question, the overall and internal structures of Colorado potato beetle lipophorin were further investigated by small-angle X-ray scattering study and compared with data obtained from cockroach and locust lipophorins.

Small-Angle X-ray Scattering Profile $I(s)$ and Intraparticle Pair-Distance Distribution Function $P(r)$. Over a temperature range from 0 to 40 °C, the independent scattering intensity profiles, $I(s)$, were determined with lipophorin solutions from the Colorado potato beetle. All profiles gave clear side maxima at $s = 0.052$ Å^{-1} ($d = 120$ Å) (Figure 2) and fairly broad ones around $s = 0.105$ Å^{-1} ($d = 60$ Å). To further analyze the temperature-dependent scattering profiles, the intraparticle pair-distance distribution function, $P(r)$, was calculated according to Katagiri et al. (1987) and illustrated in Figure 3C.

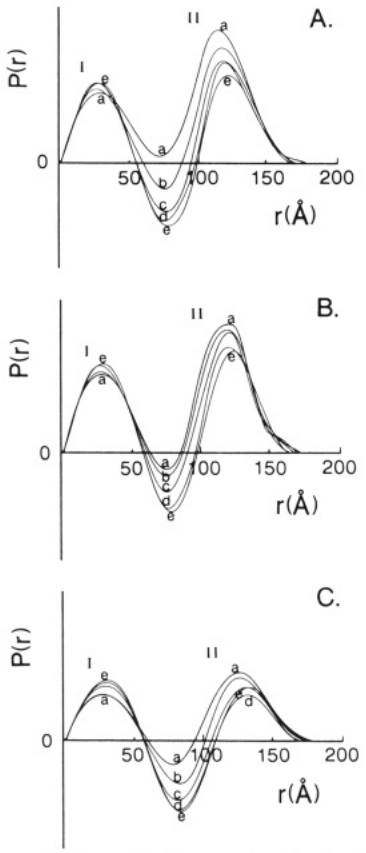

FIGURE 3: Intramolecular pair-distance distribution functions, $P(r)$, of (A) cockroach lipophorin, (B) locust lipophorin, and (C) Colorado potato beetle lipophorin calculated from the observed $I(s)$ data at temperatures from 0 to 40 °C. (a) 0 °C; (b) 10 °C; (c) 20 °C; (d) 30 °C; (e) 40 °C.

Table II: Temperature Dependence of the Radii of Gyration (R_g) and the Maximum Particle Dimensions (D_{max}) of the Colorado Potato Beetle Lipophorin

temp (°C)	R_g (Å)[a]	D_{max} (Å)[a]
0	76 (2)	180 (5)
10	78 (2)	180 (5)
20	76 (2)	170 (8)
30	73 (4)	170 (8)
40	76 (4)	175 (8)

[a] The values given in parentheses are the standard deviations obtained by a least-squares procedure.

Two distinct maxima were observed at about r = 30 and 130 Å in $P(r)$. Both maxima are affected by temperature, which indicates that the structure of lipophorin varies with the prevailing temperature.

Overall Structure. The overall structure of lipophorin was analyzed by calculating the radius of gyration, R_g, and the maximum particle dimension, D_{max}, from the $I(s)$ and $P(r)$ values at different temperatures. As shown in Table II over the range of 0–40 °C, R_g and D_{max} of lipophorin are almost identical within the experimental errors. The R_g is about 76 Å, and D_{max} is about 175 Å. Because R_g and D_{max} are not affected by temperature, the overall structure of lipophorin remains almost unchanged within this temperature range. A similar situation was observed for cockroach and locust lipophorins.

Internal Structure. The $P(r)$ of Colorado potato beetle lipophorin exhibits two distinct maxima around r = 30 and 130 Å (Figure 3C). Considering its spherical shape (diameter = 165 ± 15 Å), as observed by electron microscopy (Figure 4), the above profiles of $P(r)$ suggest that radially symmetrical

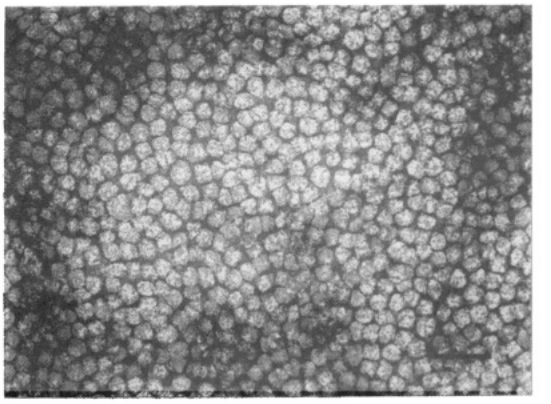

FIGURE 4: Electron micrograph of Colorado potato beetle lipophorin negatively stained with uranyl acetate at a magnification of 160 000. The bar corresponds to 500 Å.

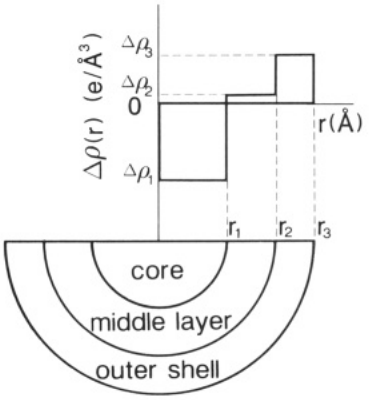

FIGURE 5: Typical radially symmetrical three-layer model used for the simulation analysis of lipophorin particle. The particle is considered to be a sphere, in which there are regions with three different electron density differences. $\Delta\rho(r)$ expressed with a step function is defined as $\Delta\rho(r) = \rho(r) - \rho_s$, where ρ_s is the electron density of solvent used.

layers with different electron densities exist inside lipophorin particles (Laggner & Müller, 1978; Pilz et al., 1979; Katagiri et al., 1987). As shown in Figure 3C, the profiles of $P(r)$ were further examined as a function of temperature. An elevation of the temperature from 0 to 40 °C significantly lowers the higher $P(r)$ peak (peak II at r = ~130 Å) and enhances the lower one (peak I at r = ~30 Å). Concomitantly, the trough between the two peaks becomes deeper. When temperatures increase, the heights of peak I do not change as much as those of peak II. Since these changes in $P(r)$ profiles are similar to those observed in cockroach and locust lipophorins (Katagiri et al., 1987), the electron densities of the layers inside Colorado potato beetle lipophorin particles seem to vary with temperature. This is further supported by the decrease in $I(0)$ values, because the overall shape and size of the particle are unaffected by temperature (Figure 2 and Table II). In addition, our DSC study of intact lipophorin also supports this conclusion, since the DSC heating curves of intact lipophorins exhibit endothermic peaks between −9 and 25 °C (Figure 1). A bigger endothermic peak centered at 16 °C coincides with changes of the profiles of $P(r)$ between 10 and 20 °C. Thus, it is strongly suggested that, unlike its overall shape, the internal structure of Colorado potato beetle lipophorin changes appreciably with temperature.

Model Building. We have built the models for lipophorins by the simulation analysis based on the $P(r)$ function. In this analysis, the functions obtained experimentally were compared with those calculated from multilayer spherical models in which the electron density distribution is expressed simply as

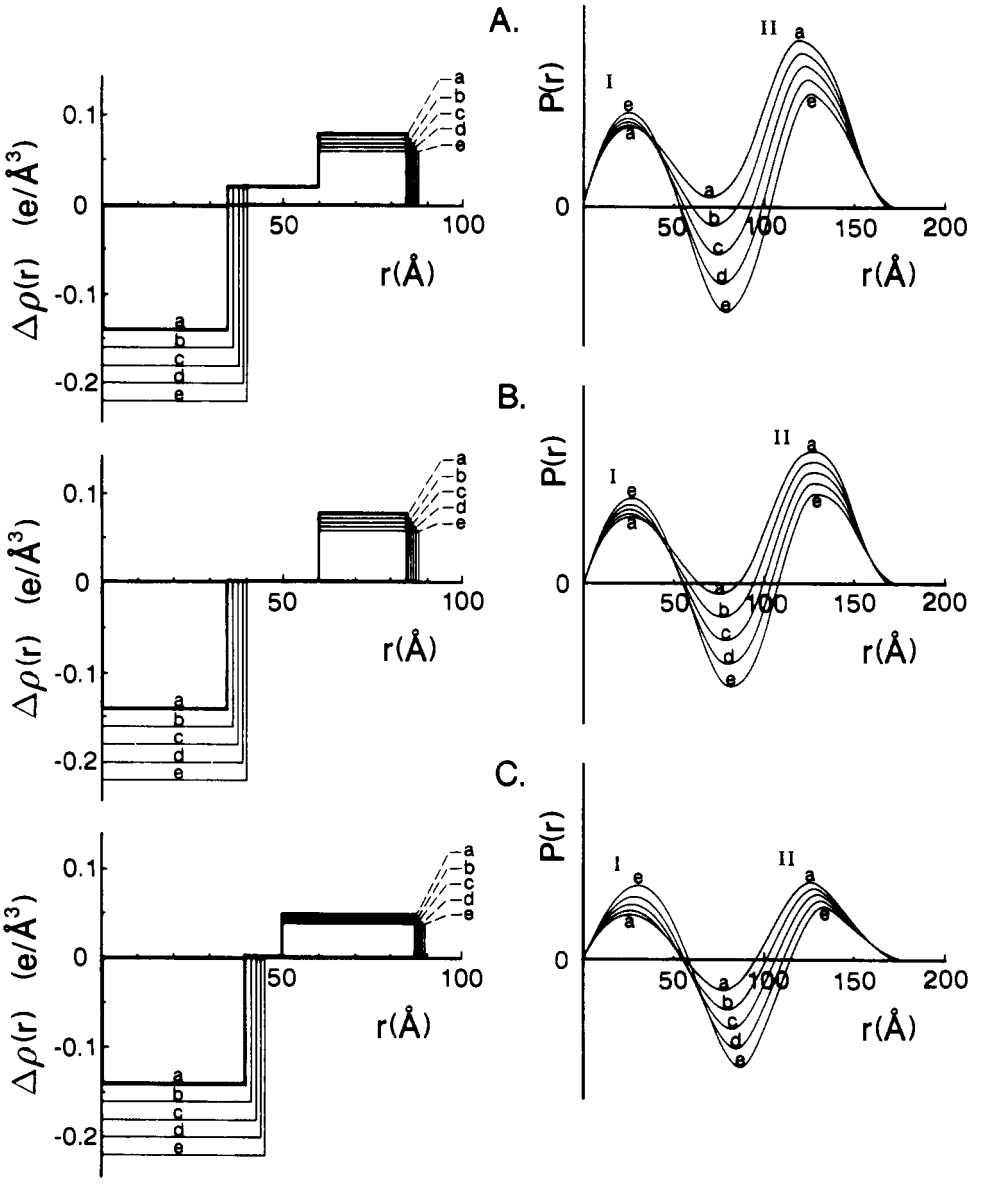

FIGURE 6: Radially symmetrical three-layer models that are best-simulated for the temperature dependence of each lipophorin particle (left) and the corresponding $P(r)$ function profiles (right). (A) Cockroach lipophorin, (B) locust lipophorin, and (C) Colorado potato beetle lipophorin. The models are expressed with the step distribution of electron density differences, $\Delta\rho(r)$ ($\rho_s = 0.34\ e/Å^3$) (Figure 5). All parameters of each model are listed in Table III.

a radially symmetrical step function (Figure 5). Since the models, however, do not always coincide with the real internal structure (electron density distribution) of the lipophorins, the simulation was ended when the models achieved qualitatively a best fit between temperature-dependent experimental and simulated $P(r)$ functions.

For cockroach and locust lipophorins, we have proposed a spherical model composed of three radially symmetrical layers with different electron densities (Figure 5). However, lipophorin from the Colorado potato beetle does not contain sufficient diacylglycerol to occupy the middle layer together with apoLp-II. This suggests that the electron density distribution inside this lipophorin may differ from those of the cockroach or the locust. Colorado potato beetle lipophorin may be a two-layered structure rather than a three-layered one. It is therefore important to elucidate the characteristic difference between the two models by using the profiles of temperature-dependent $P(r)$ functions (Igarashi et al., 1990).

For this purpose, we reconsidered the simulation of the previously proposed three-layer model of cockroach and locust lipophorins. Since the previous model was somewhat unsatisfactory in the $P(r)$ function [see Figure 5 in the paper by Katagiri et al. (1987)], we were afraid that the simulation procedure used for the previous model might lead to an incorrect estimation of the internal structure of Colorado potato beetle lipophorin. The previous simulation was performed in real space by using $P(r)$ with only r_1 and r_2 as variables (see Figure 5 for definitions). As a result, the heights of peak II of the simulated $P(r)$ functions changed inversely to those of the experimental ones. To refine the simulation model, we varied all structural parameters of the three-layer model independently (r_1, r_2, r_3, $\Delta\rho_1$, $\Delta\rho_2$, and $\Delta\rho_3$ in Table III; see Figure 5 for each definition). Figure 6A,B (left and right) show the final models for cockroach and locust lipophorins and their $P(r)$ functions obtained from the present simulation study. The improved models for cockroach and locust lipophorins are in good agreement with the experimental data (Figure 3A,B) if the following assumption is taken into account. The lipophorin particle is an ideal sphere in which the electron density distribution is radially symmetrical and expressed in a simple

Table III: Parameters of the Models in Figure 6

	parameters					
model	r_1 (Å)	r_2 (Å)	r_3 (Å)	$\Delta\rho_1$ (e/Å^3)	$\Delta\rho_2$ (e/Å^3)	$\Delta\rho_3$ (e/Å^3)
A-a	35.00	60.0	85.0	−0.14	0.02	0.080
A-b	36.25	60.0	85.5	−0.16	0.02	0.075
A-c	37.50	60.0	86.0	−0.18	0.02	0.070
A-d	38.75	60.0	86.5	−0.20	0.02	0.065
A-e	40.00	60.0	87.0	−0.22	0.02	0.060
B-a	35.00	60.0	85.0	−0.14	0	0.080
B-b	36.25	60.0	85.5	−0.16	0	0.075
B-c	37.50	60.0	86.0	−0.18	0	0.070
B-d	38.75	60.0	86.5	−0.20	0	0.065
B-e	40.00	60.0	87.0	−0.22	0	0.060
C-a	40.00	50.0	87.5	−0.14	0	0.050
C-b	41.25	50.0	88.0	−0.16	0	0.0475
C-c	42.50	50.0	88.5	−0.18	0	0.045
C-d	43.75	50.0	89.0	−0.20	0	0.0425
C-e	45.00	50.0	89.5	−0.22	0	0.040

step function. The models correspond collectively with the experimental results of peak II heights, which we failed to simulate in the previous model. Nevertheless, the present model is not fully consistent with the experimental results. D_{max} (= $2r_3$) of the model increases with increase in temperature, although D_{max} estimated from experimental $P(r)$ functions are found to be almost independent of temperature (Katagiri et al., 1987). At present, we have not further improved the simulation, because the increase in D_{max} was small compared with the experimental errors in D_{max} estimations.

We next applied this improved simulation procedure to study Colorado potato beetle lipophorin. As shown in Figure 3, the temperature dependency of the experimental $P(r)$ functions in Colorado potato beetle lipophorin looks similar to those of the other lipophorins. However, small but significant differences were observed in the temperature dependence of peaks I and II. In Colorado potato beetle lipophorin, peak I of the $P(r)$ functions is highly sensitive to changes in temperature compared with cockroach or locust lipophorin, indicating a slight difference in internal organization. From our simulation analysis using $P(r)$ functions of three-layer models, it became obvious that the changes in heights of the peaks I and II are strongly dependent on the thickness of the middle layer. The smaller the thickness of the middle layer, the more changes the ratio of the two peaks. This indicates that the middle layer plays a key role in the control of the relative heights of peaks I and II. These results were fairly informative for the subsequent simulation analysis of Colorado potato beetle lipophorin, because changes in peak I are significantly larger than in cockroach or locust lipophorins. It is therefore rather likely that a middle layer exists in Colorado potato beetle lipophorin but that its size is smaller than in cockroach or locust lipophorin.

Lipophorin Model. Simulation of the model for Colorado potato beetle lipophorin was based on the above mentioned model for cockroach and locust lipophorins. The parameters r_1 and r_3 of the model can be derived from the total volume of hydrocarbons and the maximum particle distance, D_{max}, of the lipophorin, respectively. The other parameters are defined similar to the cockroach or locust model.

To investigate the internal structure of Colorado potato beetle lipophorin at 0 °C, the initial model was subjected to simulation in real space using the $P(r)$ function. The model was further assessed by simulating the temperature effects of the experimental $P(r)$ functions. Figure 6C (left) shows that the simulation resulted in the best-fitted models of the experimental data. The profiles of the $P(r)$ calculated from the models as a function of temperature (Figure 6C, right) fitted satisfactory with the experimentally obtained functions (Figure 3C). It should be noted, however, that in Figure 6 (left) the changes of equal intervals of radius, Δr, and the differences in electron density, $\Delta\rho$, of each layer do not entirely correspond to the real temperature changes of the radii and the electron densities of lipophorin particles, because they are only qualitatively correlated with the temperature dependency of $P(r)$ functions.

The internal structure of the model thus obtained shows that an increase in temperature is well correlated with the decrease in electron density and with the increase in radius of the inner core, due to the phase transition of the hydrocarbons between −5 and 25 °C. The proposed three-layer model and its temperature-dependent change in electron density seem to reflect the structure of this lipophorin reasonably well.

The present model has an inner radius of 40–45 Å, which is slightly larger than the cockroach and locust core (35–40 Å). The outer layer (37.5–39.5 Å) is almost 1.5 times that of cockroach and locust lipophorins (25–27 Å). The middle layer (5–10 Å) is only one-fifth to half of that in the other two lipophorins (20–25 Å). Therefore, apoLp-II, which is proposed to occupy the middle layer together with diacylglycerol, may reside in both the outer and middle layers in Colorado potato beetle lipophorin. Since this lipophorin has the ability for diacylglycerol uptake from the fat body (Katagiri & de Kort, 1991), the dimension of the middle layer will be correlated with its diacylglycerol content. If this lipophorin contains variable amounts of diacylglycerol at different developmental stages, the middle layer will be larger and will contain a larger part of apoLp-II. In addition, it is possible that carotenoids, another lipid constituent, (3% of the total lipids) share the middle layer with diacylglycerol and apoLp-II, because the electron density of β-carotene (0.33 e/Å^3), one-third of the carotenoids in Colorado potato beetle lipophorin, is almost identical to that of the middle layer (Table I). Thus, we propose a three-layer model as the possible structure of lipophorin from adult Colorado potato beetle hemolymph. The outer layer is composed of phospholipid, apoLp-I, and part of apoLp-II, the middle layer of carotenoids, diacylglycerol, and the rest of apoLp-II, and the inner core of hydrocarbons. Further detailed information on the internal structure of the lipophorin will be obtained from the small-angle X-ray scattering experiments with the contrast variation method (Stuhrmann, 1974), which is now in progress.

ACKNOWLEDGMENTS

We thank Dr. E. Nagao, Hokkaido University, for taking electron micrographs and Dr. P. T. Brey, Institut Pasteur, for reading the manuscript.

Registry No. β-carotene, 7235-40-7; cholesterol, 57-88-5.

REFERENCES

Chino, H. (1985) in *Comprehensive Insect Physiology, Biochemistry, and Pharmacology* (Kerkut, G. A., & Gilbert, L. I., Eds.) Vol. 10, pp 115–134, Pergamon Press, Oxford.

Chino, H., Murakami, S., & Harashima, K. (1969) *Biochim. Biophys. Acta 176*, 1–26.

de Kort, C. A. D., & Koopmanschap, A. B. (1987) *Arch. Insect Biochem. Physiol. 5*, 255–269.

Downer, R. G. H., & Chino, H. (1985) *Insect Biochem. 15*, 627–630.

Edelstein, C. Kẽzdy, F. J., Scanu, A. M., & Shen, B. W. (1979) *J. Lipid Res. 20*, 143–153.

Goldstein, J. L., Brown, M. S., Anderson, R. G. W., Russel, D., & Schneider, W. J. (1985) *Rev. Cell Biol. 1*, 1–39.

Guinier, A., & Fournet, G. (1955) *Small-Angle Scattering of X-Rays*, p 126, John Wiley and Sons, New York.
Igarashi, T., Sato, M., Katsube, Y., Takio, K., Tanaka, T., Nakanishi, M., & Arata, Y. (1990) *Biochemistry 29*, 5727-5733.
Kashiwazaki, Y., & Ikai, A. (1985) *Arch. Biochem. Biophys. 237*, 160–169.
Katagiri, C. (1985) *Biochim. Biophys. Acta 834*, 139–143.
Katagiri, C., & Chino, H. (1973) *Insect Biochem. 3*, 429–437.
Katagiri, C., & de Kort, C. A. D. (1991) *Comp. Biochem. Physiol., B: Comp. Biochem.* (in press).
Katagiri, C., Kimura, J., & Murase, N. (1985) *J. Biol. Chem. 260*, 13490–13495.
Katagiri, C., Sato, M., & Tanaka, N. (1987) *J. Biol. Chem. 262*, 15857–15861.
Laggner, P., & Müller, K. W. (1978) *Q. Rev. Biophys. 11*, 371–425.
Pilz, I., Glatter, O., & Kratky, O. (1979) *Methods Enzymol. 61*, 175.
Robbs, S. L., Ryan, R. O., Schmidt, J. O., Keim, P. S., & Law, J. H. (1985) *J. Lipid Res. 26*, 241–247.
Shapiro, J. P., Keim, P. S., & Law, J. H. (1984) *J. Biol. Chem. 259*, 3680–3685.
Shapiro, J. P., Law, J. H., & Wells, M. A. (1988) *Annu. Rev. Entomol. 33*, 297–318.
Stuhrmann, H. B. (1974) *J. Appl. Crystallogr. 7*, 173–178.

Fourier Transform Infrared Spectroscopic Studies of Ca^{2+}-Binding Proteins†

Michael Jackson,*,‡ Parvez I. Haris,§ and Dennis Chapman§

Steacie Institute for Molecular Sciences, National Research Council of Canada, Ottawa, Ontario K1A 0R6, Canada, and Department of Protein and Molecular Biology, Royal Free Hospital School of Medicine, Rowland Hill Street, London NW3 2PF, U.K.

Received January 28, 1991; Revised Manuscript Received June 14, 1991

ABSTRACT: The secondary structures of calmodulin and parvalbumin are well established from X-ray diffraction and nuclear magnetic resonance spectroscopic studies, which indicate that these proteins are predominantly α-helical in character. Recent infrared studies have nevertheless suggested that the helical structures present in these proteins in solution are not the standard α-helix but rather some kind of distorted helices [Trewhella, J., et al. (1989) *Biochemistry 28*, 1294]. The evidence for this was the unusually low amide I frequency for calmodulin and troponin C in ^2H_2O solution. The studies presented here, however, suggest that the helical structures in these proteins are not significantly distorted, for two reasons. First, distorted helical structures have weaker hydrogen bonds than the standard α-helix and would therefore be expected to absorb at a higher rather than a lower frequency. Second, distorted helical structures would absorb at an unusual frequency in H_2O solutions which is not the case for the proteins studied here. The band frequency of these proteins is observed to occur at a frequency observed with other proteins known to contain predominantly α-helical structures. Quantitative analysis of the FT-IR spectra of calmodulin (67% α-helix) and parvalbumin (68% α-helix) in H_2O in the presence of Ca^{2+} gives helical contents similar to those reported by X-ray studies. This raises the question as to why these proteins in H_2O show a normal frequency for the presence of α-helical structures and an abnormal frequency in ^2H_2O. Addition of deuterated glycerol to the proteins in ^2H_2O solutions results in a significant shift of absorbance to higher frequency. This is consistent with dehydration of the protein taking place. Circular dichroism spectra of the proteins in glycerol show no evidence of any structural rearrangements. The unusually low amide frequency for these proteins in ^2H_2O is interpreted on the basis of an unusual degree of solvent interaction with exposed helical structures, lowering the amide I maximum only in ^2H_2O due to the increased strength of deuterium bonds as compared to hydrogen bonds. Quantitative analyses of FT-IR spectra of calmodulin and parvalbumin show an increase in the helical content by approximately 6% for both proteins on addition of Ca^{2+}. A reduced rate of hydrogen–deuterium exchange in the Ca^{2+}-loaded state suggests the formation of a more compact structure. The most marked effect of Ca^{2+} is an enhanced thermal stability of these proteins. Elevation of the temperature to 70 °C in the absence of Ca^{2+} results in disruption of helical structures and formation of an intermolecular β-sheet. This rearrangement is prevented by Ca^{2+}.

Many cytosolic proteins are targeted by Ca^{2+}. Of these, the so-called EF-hand proteins are by far the most widely studied. These are a homologous family of proteins containing the recurring helix–loop–helix or EF-hand structural motif described by Kretsinger and Nockolds (1973). Two helices are separated by a loop containing around 12 amino acids, many of which are acidic and are involved in Ca^{2+} coordination. The helices are oriented approximately perpendicular to each other.

The first EF-hand protein to be crystallized was parvalbumin (Kretsinger & Nockolds, 1973). Parvalbumin was shown by X-ray diffraction (Moews & Kretsinger, 1975) to consist of six α-helical regions, labeled A–F, helices A and B, C and

† This work was supported by the Wellcome Trust.
* To whom correspondence should be addressed.
‡ National Research Council of Canada.
§ Royal Free Hospital School of Medicine.

0006-2960/91/0430-9681$02.50/0